

# Reaction of state-selected ammonia ions with methane

Michael A. Everest, John C. Poutsma, Jonathan E. Flad, and Richard N. Zare<sup>a)</sup>

*Department of Chemistry, Stanford University, Stanford, California 94305*

(Received 19 April 1999; accepted 18 May 1999)

We have investigated the reaction of ammonia ions with methane molecules ( $\text{CD}_4$ ) over the collision energy range of 0.5–10.0 eV and for ammonia ion vibrational states ranging from  $\nu_2 = 1-10$ . Under these conditions, the two main product channels are  $\text{NH}_3\text{D}^+$  and  $\text{CD}_3^+$ . The cross section for formation of  $\text{NH}_3\text{D}^+$  is enhanced with increasing internal energy at collision energies below 6.0 eV, and independent of internal energy at higher collision energies. The enhancement is greater for forward-scattered products indicating that ammonia-ion vibrational energy enhances reactivity at large impact parameters. The mechanism for formation of  $\text{CD}_3^+$  involves collision-induced dissociation of  $\text{CD}_4$  (or  $\text{NH}_3^+$ ) which leads to the formation of a short-lived  $[\text{NH}_3\text{CD}_3]^+$  ( $[\text{NH}_2\text{CD}_4]^+$ ) complex, which then decays to products. This reaction is found not to be vibrationally mode selective, which is consistent with the hypothesis that mode selectivity in reactions of ammonia ions is driven by the Franck–Condon overlap whenever charge transfer is involved. © 1999 American Institute of Physics. [S0021-9606(99)02130-3]

## I. INTRODUCTION

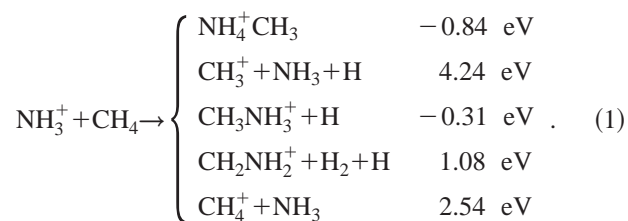
We have studied the effects of different types of energy on the reactivity of ammonia ions with methane molecules to understand better the dynamics of ion-molecule reactions. Information regarding the microscopic dynamics of the reaction is deduced by investigating the effects of collision energy, ion internal energy, and ion vibrational state on reaction efficiency, product branching, and product scattering.

The ammonia ion/methane system is of interest for several reasons. First, the reaction system has only two heavy atoms, so that it serves to test the best contemporary theories of ion-molecule reaction dynamics. Second, the ammonia ion is one of the few that can be prepared in a wide variety of specific internal states owing to the nature of the ionization scheme employed.<sup>1</sup> Finally, methane is isoelectronic both with neutral ammonia, previously observed to react in a mode-selective manner,<sup>2</sup> and with neutral water, previously observed not to react mode selectively.<sup>3</sup> The ammonia ion/methane system therefore is a test case for understanding the necessary and sufficient criteria of mode selectivity in ion-molecule reactions.

This system has not been investigated in detail in the past. The thermal rate constant for the reaction of  $\text{NH}_3^+ + \text{CD}_4 \rightarrow \text{NH}_3\text{D}^+ + \text{CD}_3$  was measured by Huntress *et al.*,<sup>4,5</sup> and was found to be  $3.9 \times 10^{-10} \text{ cm}^3 \text{ mol}^{-1} \text{ s}^{-1}$ . They observed no other product channels from this reaction. The only state-selected study to date is that of Conaway, Ebata, and Zare.<sup>6</sup> They measured the reactivity of  $\text{NH}_3^+ + \text{CH}_4$  as a function of both collision energy and ammonia  $\nu_2$  bending. The observed ionic products include the following:  $\text{NH}_4^+$  from direct atom abstraction,  $\text{CH}_3^+$ ,  $\text{CH}_3\text{NH}_3^+$ , and  $\text{CH}_2\text{NH}_2^+$ . While they claim the latter condensation products to be direct products of the reaction, we sus-

pect they were products resulting from multiple collisions, as their experiments were done at much higher pressures than the present work.

Equation (1) shows the energetics of selected product channels



The energies reported are  $\Delta H_{\text{rxn}}$  at 298 K.<sup>7</sup> Note that these reactions and energetics involve only hydrogen atoms, whereas the experiments discussed below involve hydrogenated ammonia and deuterated methane.

## II. EXPERIMENTAL METHOD

The experimental method employed is described more fully elsewhere;<sup>8,9</sup> only a brief description is given here. Ammonia ions are prepared in selected vibrational states with (2+1) resonance-enhanced multiphoton ionization<sup>1</sup> (REMPI) of ammonia in a pulsed molecular beam. This scheme is used to prepare ammonia ions with 0 or 1 quanta in the  $\nu_1$  symmetric stretching (“breathing”) mode and 0–10 quanta of vibrational energy in the  $\nu_2$  symmetric bending (“umbrella”) mode.<sup>10,11</sup> A particular vibrational preparation is described as  $1^m 2^n$  for  $m$  quanta in the  $\nu_1$  mode and  $n$  quanta in the  $\nu_2$  mode. If  $m=0$  only  $2^n$  may be specified. The ions are extracted orthogonally from the molecular beam and injected into a quadrupole mass filter that passes only ions with a mass-to-charge ratio of the desired reactant ion. The reactant ion beam then passes through a collimating lens and into an octopole ion guide<sup>12</sup> in which the reactive collisions occur. The presence of the ion guide ensures the col-

<sup>a)</sup> Author to whom correspondence should be addressed; electronic mail: zare@stanford.edu

lection of all products, regardless of scattering angle.<sup>8</sup> The neutral collision gas (methane-*d*4, CIL, 99% D, lot 94-1) is introduced through a leak valve into a short collision cell that is concentric with the octopole ion guide.

The reaction collision energy is experimentally controlled by varying the dc float voltage of the octopole ion guide. The voltage of the field-free ionization region is kept constant at 6.00 V. Changing the octopole dc float voltage from 5.08 to -12.50 V corresponds to changing the center-of-mass collision energy range from 0.50 to 10.0 eV. The product ions and unreacted ammonia ions drift through the octopole and are mass selected with a second quadrupole. Time-of-flight profiles for reactants and products are then recorded simultaneously with a multichannel scaler and a current transient recorder.

We report relative integral cross sections that are calculated by normalizing the counted signal for the product in question to the integrated current of the reactant ion. Here "relative" refers to the fact that we are unable to measure absolute cross sections because we know neither the exact pressure in the collision cell nor the effective path length. Although the units are arbitrary, all of the cross sections reported in the present work may be compared with each other, as the pressure in the collision cell was kept nearly constant (*vide infra*) for all the experiments. We also report product branching ratios that are defined as the intensity of a particular product normalized by the total product intensity under the same experimental conditions. Although branching ratios contain less information than relative cross sections (i.e., a change in branching ratio does not indicate which product became more intense or which lost intensity), they have the advantage of being invariant to any experimental error that has an equal multiplicative effect on all products. Examples of such errors may include the integral of the collision cell pressure over the cell path length, or any nonlinear process in the estimation of reactant intensity.

The estimated pressure in the collision cell ranged between 65 and 85  $\mu$ Torr with most experiments being done with a collision cell pressure of 75  $\mu$ Torr. (These values are highly uncertain.) To ensure single-collision conditions, the branching ratios for the various products were measured over a broad collision-cell pressure range (roughly 16–810  $\mu$ Torr) and were found to be independent of pressure.

The possibility of signal arising from sources other than reactions in the collision cell was checked at all collision energies by repeating the experiment without introducing CD<sub>4</sub> into the reaction chamber. These experiments were performed with the ammonia ion in the 2<sup>2</sup> and 2<sup>3</sup> vibrational states. The background cross section to form a mass-to-charge ratio of 19 was always insignificant (corresponding to <3, arbitrary units). The background cross sections were found to be somewhat higher for an ion having a mass-to-charge ratio of 18, but were practically zero even in this case (5 at 0.5 eV, 20 at 4.0 eV, and 7 at 10.0 eV). Most trends in the data that are discussed below involve changes of the relative cross sections by several hundred units. Although insignificant, we suspect this background to be ions formed from reaction either with ambient CD<sub>4</sub> in the chamber to form CD<sub>3</sub><sup>+</sup> or a hydrogen abstraction reaction from hydrocar-

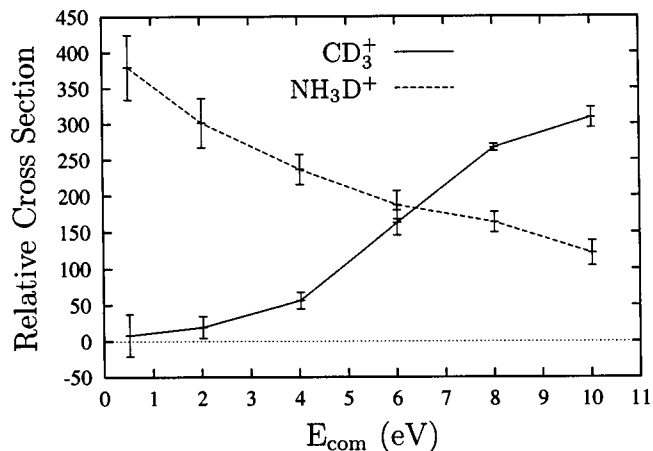


FIG. 1. Relative reaction cross sections (arbitrary units) for the reaction  $\text{NH}_3^+(1^0_2^5) + \text{CD}_4$  as a function of center-of-mass frame collision energy ( $E_{\text{com}}$ /eV) to form the two observed products:  $\text{NH}_3\text{D}^+$  and  $\text{CD}_3^+$ . The lines represent the mean of the four data sets included in the figure, and the error bars represent twice the standard deviation ( $\pm 2s$ ).

bon species (e.g., pump oil fragments) in the chamber to form  $\text{NH}_4^+$ .

Because the experiment is initiated with a short laser pulse ( $\approx 10$  ns), and the detector is time sensitive ( $\tau < 5$  ns), the time of flight of the products can also be measured, yielding some indication of the differential reaction cross section. The instrument function is estimated by simulating the guided-ion beam to determine the correlation between ion flight time and ion velocity in the octopole. The reactant and product time-of-flight profiles are then transformed into the velocity domain. Product signal can be plotted as an histogram versus the projection of the product velocity onto the octopole axis (i.e.,  $w_p \cos(\theta)$  where  $w_p$  is the product velocity in the center-of-mass frame and  $\theta$  is the scattering angle). The instrument axis is coincident with the initial velocity of the ammonia-ion reactant, and therefore, the average velocity of the center of mass. Although the complete differential scattering cannot be deduced from these histograms [i.e., separation of the  $w_p$  and  $\cos(\theta)$ ], information regarding the degree of forward or backward scattering is obtained.

The raw transformed data are binned into 100-m/s-wide bins—much smaller than the instrumental blurring. A sharply increasing feature toward low velocity (zero in the laboratory frame, to be precise) in the velocity profiles arises from random dark current at very long times or very slow ions. As the velocity approaches zero, the amount of time contributing to each velocity bin increases dramatically yielding this spurious feature.

### III. RESULTS AND DISCUSSION

#### A. $\text{NH}_3\text{D}^+$

##### 1. Collision energy dependence

Figure 1 shows the collision energy dependence of the relative reaction cross section for the two observed channels. These data are for the reaction of  $\text{NH}_3^+(1^0_2^5) + \text{CD}_4$ . The major products for this reaction have masses of 18 and 19 amu,

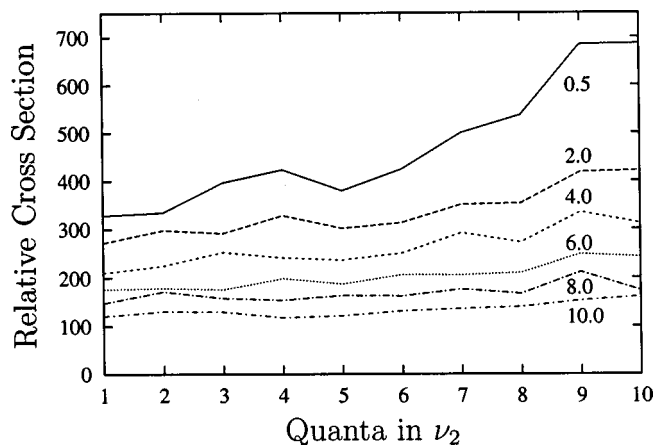


FIG. 2. Relative reaction cross sections (arbitrary units) for the formation of  $\text{NH}_3\text{D}^+$  (deuterium abstraction) as a function of ammonia-ion vibrational state (quanta in  $\nu_2$ ) for center-of-mass collision energies from 0.5 to 10.0 eV. The vibrational spacing is 0.12 eV, so the internal energy spanned by the plot is from 0.12 to 1.2 eV. Each curve represents the average of at least three experiments.

corresponding to dissociative charge transfer ( $\text{CD}_3^+$ ) (see Sec. III B, below) and deuterium abstraction ( $\text{NH}_3\text{D}^+$ ), respectively. The relative cross section for the deuterium abstraction is seen to drop by more than a factor of 3 upon increasing the center-of-mass collision energy from 0.5 to 10 eV.

Conaway, Ebata, and Zare<sup>6</sup> observed the same product channel from this reaction, however it was not seen to decrease at the higher collision energies. We suspect that this difference may be caused by the fact that they used static ion optics to guide the products to the detector, whereas the present apparatus uses an rf octopole ion guide. Without the trapping abilities of the octopole the collection efficiency may have been drastically higher for faster products than for the slower products formed at the lower collision energies (see Sec. III 3 and Fig. 4, below). This behavior could cause the apparent discrepancy.

This reaction channel is very similar to the corresponding channel observed in the reaction of the ammonia ion with molecular hydrogen ( $\text{NH}_3^+ + \text{D}_2 \rightarrow \text{NH}_3\text{D}^+ + \text{D}$ ).<sup>13</sup> The main difference between the present system and the analogous reaction with  $\text{D}_2$  is that the cross section for the latter increases between  $E_{\text{com}} = 0.5$  eV and  $E_{\text{com}} = 4.0$  eV, whereas the former monotonically decreases over the entire collision energy range. This trend could indicate that the intrinsic reaction coordinate for atom abstraction from molecular deuterium involves a significant barrier in approaching the transition state, whereas no such entrance barrier (or a much smaller barrier) exists for atom abstraction from methane.

That the cross section drops off at higher collision energies is likely caused simply by the total collision cross section falling off, which is consistent with the Langevin model.

## 2. Internal energy dependence

Figure 2 shows the dependence of the relative reaction cross section to form  $\text{NH}_3\text{D}^+$  on the ammonia-ion vibrational state (i.e., on  $\nu_2$ , the umbrella bending mode) for all colli-

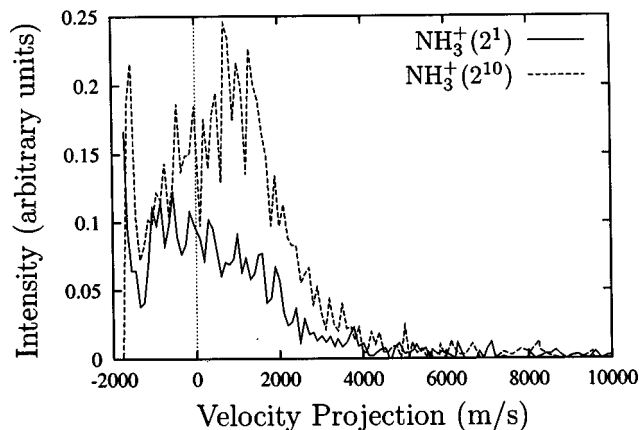


FIG. 3. Center-of-mass frame velocity histograms for  $\text{NH}_3\text{D}^+$  coming from reactions with  $\text{NH}_3^+(2^1)$  and  $\text{NH}_3^+(2^{10})$ . The collision energy is 0.5 eV (com) for both curves. Each curve represents the binned (100 m/s) average of three experiments.

sion energies studied ( $E_{\text{com}} = 0.5$ –10.0 eV). Ammonia-ion internal excitation ranged from  $\nu_2 = 1$ –10 (total internal energy:  $E_{\text{int}} = 0.12$ –1.2 eV). Deuterium abstraction is enhanced with increasing energy in the  $\nu_2$  bending mode. This enhancement is greatest (a factor of 1.95 from  $\nu_2 = 1$  to  $\nu_2 = 10$ ) at the lowest collision energy studied (0.5 eV), and decreases gradually with increasing collision energy. The enhancement is immeasurably small at collision energies above 6.0 eV.

It is tempting to ascribe this vibrational enhancement to the fact that  $\nu_2$  motion in the ion is along the intrinsic reaction coordinate for deuterium abstraction (i.e., the planar reactant ion moving toward the tetrahedral  $\text{NH}_3\text{D}^+$  product). However, as is demonstrated in Sec. III C, below, the effect is only owing to the internal energy, not specific vibrational motion (normal mode) of the molecule.

That internal energy enhances reactivity, whereas collision energy has an inhibiting effect, is consistent with a late barrier on the potential energy surface of this chemical system, though we hesitate to make any strong claims regarding the details of this system.

## 3. Product scattering

*a. Vibrational enhancement of  $\text{NH}_3\text{D}^+$ .* While Fig. 2 shows how the integral reaction cross section to form  $\text{NH}_3\text{D}^+$  depends on  $\nu_2$  excitation, Fig. 3 and Table I reveal some angular dependence of this enhancement. The figure shows the velocity histogram for  $\text{NH}_3\text{D}^+$  from reactions with

TABLE I. Vibrational enhancement in the forward and backward directions for the reaction of  $\text{NH}_3^+(2^n) + \text{CD}_4 \rightarrow \text{NH}_3\text{D}^+ + \text{CD}_3$  derived from the appropriate integrals of the data shown in Fig. 3. The units for the rows labeled 2<sup>1</sup> and 2<sup>10</sup> are arbitrary cross section intensity units. The enhancements are unitless ratios.

$\text{NH}_3^+$ state	Forward	Backward	Total
2 <sup>1</sup>	209.4	149.0	358.4
2 <sup>10</sup>	470.7	229.1	699.8
Enhancement	2.25	1.54	1.95

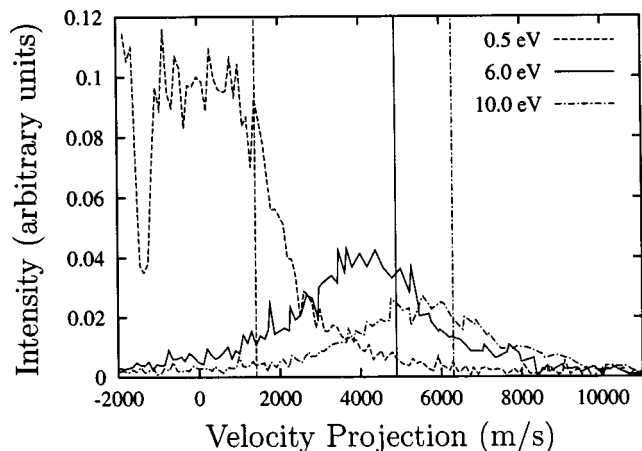


FIG. 4. Center-of-mass frame velocity histograms for  $\text{NH}_3\text{D}^+$  as a function of collision energy. Each curve represents the binned (100 m/s) average of 16 experiments. The vertical lines indicate the prediction of the spectator-stripping assumption.

$\text{NH}_3^+(2^1)$  and  $\text{NH}_3^+(2^{10})$ . The center-of-mass collision energy is 0.5 eV for both reactions; the collision energy at which the highest vibrational enhancement is observed. Table I quantitatively shows that the vibrational enhancement seen in Fig. 2 is predominantly from enhancement in the forward-scattered products. This enhancement in the forward direction suggests that at low collision energy (such as 0.5 eV) increasing internal energy in the ammonia ion changes the opacity function [ $P(b)$ , the probability of reaction as a function of impact parameter] such that higher impact parameters lead to reaction.

*b. Scattering of  $\text{NH}_3\text{D}^+$ .* Inspection of Fig. 2 shows that the integral cross section is independent of ammonia-ion vibrational state over the range of  $\nu_2 = 1-5$ . The corresponding velocity profiles (not shown) confirm that the scattering is also independent of  $\nu_2$  excitation over this range. For these reasons it is justifiable to average together velocity profiles from experiments involving these different ammonia ion preparations. This procedure affords a superior signal-to-noise ratio in the velocity data as it permits the averaging of many more experiments (16 total).

The dependence of  $\text{NH}_3\text{D}^+$  scattering on collision energy is shown in Fig. 4. The vertical lines indicate the prediction of the spectator-stripping model according to which the velocity of the  $\text{CD}_3$  fragment is assumed not to change through the course of the collision. This value is calculated according to

$$w_{\text{NH}_3\text{D}^+} = \frac{m_{\text{CD}_3}}{m_{\text{NH}_3\text{D}^+}} \sqrt{\frac{2E_{\text{com}} m_{\text{NH}_3\text{D}^+}}{M m_{\text{CD}_4}}},$$

where  $m_i$  is the mass of species  $i$  in kilograms,  $w_i$  is the center-of-mass frame velocity of species  $i$  in meters per second, and  $M$  is the total mass of the system in kilograms. The experimentally determined velocity profiles are seen to scatter predominantly in the forward direction—approaching the spectator stripping limit. The contraction of the integral reaction cross section with increasing collision energy (seen in Fig. 1) is also clear.

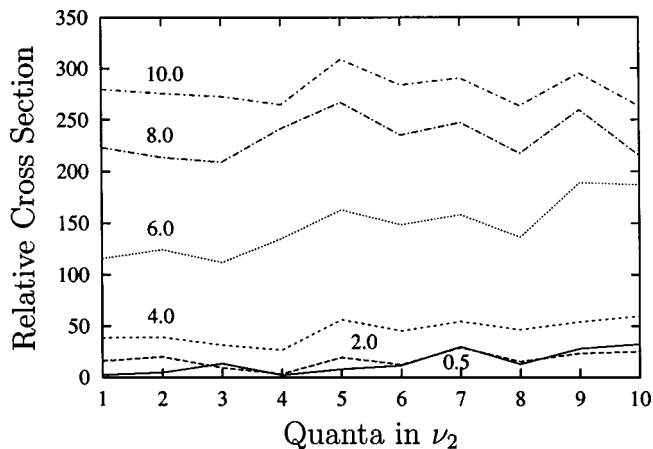


FIG. 5. Relative reaction cross sections (arbitrary units) for the formation of  $\text{CD}_3^+$  (dissociative charge transfer) as a function of ammonia-ion vibrational state (quanta in  $\nu_2$ ) for center-of-mass collision energies from 0.5 to 10.0 eV. The vibrational spacing is 0.12 eV, so the internal energy spanned by the plot is from 0.12 to 1.2 eV. Each curve represents the average of at least three experiments.

This scattering behavior is typical of ion-molecule reactions in which large impact parameter collisions are frequent owing to the strong electrostatic forces involved (charge/induced dipole in this case). This behavior is similar to the spectator-stripping scattering observed in the reaction  $\text{NH}_3^+ + \text{D}_2\text{O} \rightarrow \text{D}_2\text{OH}^+ + \text{OD}$ .<sup>3</sup> In the latter case, however, the  $\text{NH}_2$  moiety was the spectator, and the ionic product scattered backward in the laboratory frame.

## B. $\text{CD}_3^+$

### 1. Collision energy dependence

The relative cross section to form  $\text{CD}_3^+$  shown in Fig. 1 is negligible at low center-of-mass collision energy, but increases dramatically at energies greater than 4.0 eV. This behavior indicates a reaction with a threshold between 2 and 5 eV. This threshold value is consistent with the reaction  $\text{NH}_3^+ + \text{CD}_4 \rightarrow \text{NH}_3 + \text{CD}_3^+ + \text{D}$  ( $\Delta H_{\text{rxn}} = 4.24$  eV). Collision energy spread could cause the products appearing at nominal energies below the thermodynamic threshold. This observation is in agreement with the previous investigation of Conway, Ebata, and Zare.<sup>6</sup>

A product channel showing similar collision energy dependence has been seen in the reaction of ammonia ion with both  $\text{D}_2\text{O}^3$  and  $\text{D}_2$ .<sup>13</sup> In the former case the mechanism giving rise to the  $\text{NH}_2\text{D}^+$  product was determined to be a two-step process: collision-induced dissociation of the ammonia ion resulting in the formation of a  $[\text{NH}_2\text{D}_2\text{O}]^+$  complex which would decay to the formal isotope exchange product. In the reaction of ammonia ion with molecular hydrogen the precise mechanism was not determined, but was thought to be either a mechanism similar to the ammonia ion/water  $\text{NH}_2\text{D}^+$  mechanism, or to be a stripping event followed by decay of the resulting  $\text{NH}_3\text{D}^+$  product.

### 2. Internal energy dependence

Figure 5 shows the dependence of the relative reaction cross section to form  $\text{CD}_3^+$  on the ammonia-ion vibrational

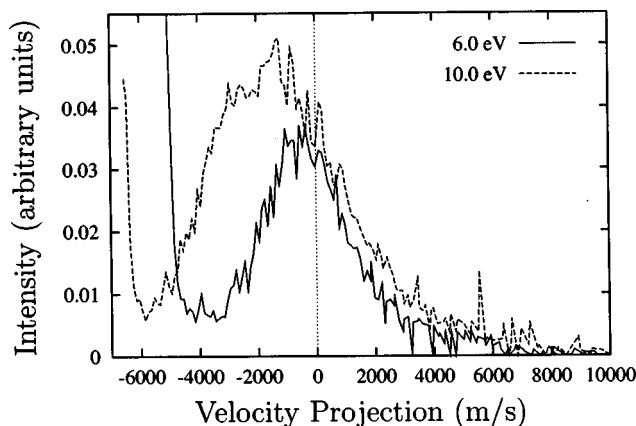


FIG. 6. Center-of-mass frame velocity histograms for  $\text{CD}_3^+$  as a function of collision energy. Each curve represents the average of 33 experiments.

state, similar to Fig. 2 (see Sec. III 2 for experimental details). The total internal energy ranges from 0.12 to 1.2 eV. Although there is little systematic effect of internal energy on the cross section at the highest and lowest collision energies investigated, there is a clear enhancement of the cross section with increasing internal energy at 6.0 eV (com)—the energy at which collision energy is also seen to have the greatest effect. The slope of a straight line fit to the 6.0 eV points in Fig. 5 is  $64 \pm 14$  cross section units per eV. This dependence is similar to the collision energy enhancement at 6.0 eV as seen in Fig. 1 ( $\approx 53$  cross section units per eV for a straight line fit between 4 and 8 eV). Therefore, collision energy and energy in the  $\nu_2$  vibrational mode of the reactant ion are equally potent in overcoming the barrier involved in this channel.

### 3. Product scattering

As was the case with  $\text{NH}_3\text{D}^+$  (see Sec. III 3), it is justifiable to average together the velocity histograms for  $\text{CD}_3^+$  from several vibrational preparations of the ammonia ion. Comparison of the individual velocity histograms (not shown) confirms that the shape of the  $\text{CD}_3^+$  velocity profiles is independent of vibrational excitation over the range of  $\nu_2 = 1 - 10$ . The following figures, therefore, contain velocity histograms that are the average of 33 individual experiments from these different ammonia-ion preparations.

Figure 6 shows the velocity profile for the  $\text{CD}_3^+$  product as it changes with collision energy. In stark contrast to the scattering of  $\text{NH}_3\text{D}^+$ , it generally scatters close to the center of mass, tending to the backward direction for high collision energies. For the reaction at  $E_{\text{com}} = 10.0$  eV the most probable velocity projection is  $v_{\text{max}} = -1254$  m/s which corresponds to 0.29 eV of energy in the center-of-mass frame. The full width at half maximum value ranges from  $-4067$  m/s (3.0 eV, com) to  $1064$  m/s (0.21 eV, com). Sixty eight percent of the  $\text{CD}_3^+$  products scatter within this range. These energy estimations should be considered only rough estimates. They assume that the measured products arise from reactions having two products (i.e., a two-body system).

The scattering behavior (Fig. 6) and the high apparent threshold (Fig. 1) for this reaction are strong evidence that

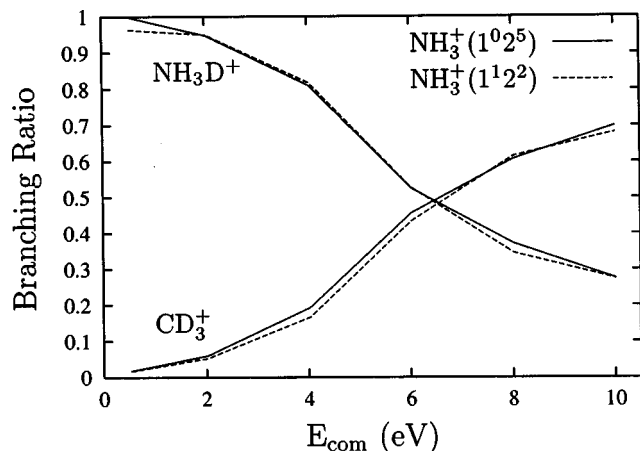


FIG. 7. Product branching ratios as a function of collision energy. Reactions of both  $\text{NH}_3^+(1^0_2^5)$  ( $E_{\text{int}} = 0.60$  eV) and  $\text{NH}_3^+(1^1_2^2)$  ( $E_{\text{int}} = 0.63$  eV) are shown.

the mechanism of formation of  $\text{CD}_3^+$  is similar to the formation of  $\text{NH}_2\text{D}^+$  from the reaction of  $\text{NH}_3 + \text{D}_2\text{O}$ . Specifically, it is likely formed by collision-induced dissociation of the ammonia ion or methane molecule, resulting in a short-lived complex ( $[\text{NH}_2\text{CD}_4]^+$  or  $[\text{NH}_3\text{CD}_3]^+$ , respectively). This complex then goes on to form  $\text{CD}_3^+$  and  $\text{NH}_2\text{D}$  or  $\text{NH}_3$ . We are unable to differentiate between these two mechanisms because we cannot detect the neutral products.

We are unable to estimate the lifetime of the complex, although the forward-backward symmetry of the product scattering in the center-of-mass frame at a collision energy of 6 eV (solid line in Fig. 4) suggests that a complex has been formed. The complex lifetime is not sufficiently long to permit any scrambling of isotopes. That is, in the isotopic variant reaction  $\text{ND}_3^+ + \text{CH}_4$  there was no detectable  $\text{CH}_2\text{D}^+$ ,  $\text{CHD}_2^+$ , or  $\text{CD}_3^+$ , only  $\text{CH}_3^+$ . Moreover, that the product is slightly backward scattered at the highest collision energies investigated indicates that the complex may be osculating (i.e., the lifetime of the complex is less than a typical rotational period) at the highest collision energy.

### C. Mode selectivity

Figure 7 compares the reactivity of two distinct, nearly isoenergetic, preparations of the ammonia ion. The product branching ratios for each product are shown as a function of center-of-mass frame collision energy. Two curves are shown for each product: one for the reaction of  $\text{NH}_3^+(1^0_2^5)$  ( $E_{\text{int}} = 0.60$  eV) and one for the reaction of  $\text{NH}_3^+(1^1_2^2)$  ( $E_{\text{int}} = 0.63$  eV). The superimposition of these two sets of curves demonstrates that there is no measurable vibrational mode-selective effect between the umbrella-bending and symmetric stretching in this system at these collision energies.

This behavior indicates that, for the collision energies investigated, the reaction of ammonia ions with methane molecules is not sensitive to the specific motion of the nuclei, only to the total amount of internal energy available. This example is the third reaction of ammonia ions (reactions with water<sup>3</sup> and molecular hydrogen<sup>13</sup> being the other two)

that is shown to have direct channels sensitive to the amount of energy in ammonia-ion vibration, but insensitive to the specific normal mode in which that energy occurs. These three reactions stand in contrast to the reactions of ammonia ions with ammonia molecules<sup>2</sup> and methanol<sup>14</sup> which show differing reactivity of  $\text{NH}_3^+(1^1 2^2)$  and  $\text{NH}_3^+(1^0 2^5)$  in some cases.

It is likely more than a mere coincidence that all of the ammonia-ion reactions demonstrating mode-selective behavior involve a charge transfer channel. We have previously proposed<sup>3</sup> that the mode selectivity observed in these reactions arises from the large Franck–Condon overlap between  $\nu_2$ -vibrationally excited  $\text{NH}_3^+$  reactant and the neutral  $\text{NH}_3$  product involved in a charge transfer reaction. It seems that the same underlying principle that allows the high- $\nu_2$  excitation of the reactant may also be the driving force behind the fascinating observed trends in reactivity.

#### IV. CONCLUSIONS

The reaction of ammonia ions with methane molecules has two predominant product channels in the collision energy range of 0.5–10.0 eV:  $\text{NH}_3\text{D}^+$  and  $\text{CD}_3^+$ .  $\text{NH}_3\text{D}^+$  is thought to be formed from a direct deuterium abstraction from methane. This process is enhanced with increasing internal energy at collision energies below 6.0 eV, and independent of internal energy at higher collision energies. The enhancement is greater for forward-scattered products indicating that ammonia-ion vibrational energy enhances the opacity function at large impact parameters (for low collision energy reactions). There is also reason to believe that this process involves a late barrier along the intrinsic reaction coordinate. The formation of  $\text{CD}_3^+$  likely arises from a mechanism involving collision-induced dissociation of  $\text{CD}_4$  (or  $\text{NH}_3^+$ ) which leads to the formation of a short-lived  $[\text{NH}_3\text{CD}_3]^+$  ( $[\text{NH}_2\text{CD}_4]^+$ ) complex. This complex then de-

cays to products. The fact that this reaction is not mode selective under these conditions supports the previously proposed hypothesis<sup>3</sup> that mode selectivity in reactions of ammonia ions is driven by the Franck–Condon overlap involved in a charge transfer channel when it is present. Experiments are under way to test this hypothesis by probing the potential mode selectivity of ammonia-ion reactions known to have efficient charge transfer channels.

#### ACKNOWLEDGMENTS

M.A.E. has been supported by an Elf Atochem Fellowship. The authors gratefully acknowledge the financial support of the Air Force Office of Scientific Research (Grant No. F49620-92-J-0074).

- <sup>1</sup>S. L. Anderson, *Adv. Chem. Phys.* **82**, 177 (1992).
- <sup>2</sup>R. D. Guettler, G. C. Jones, L. A. Posey, and R. N. Zare, *Science* **266**, 259 (1994).
- <sup>3</sup>M. A. Everest, J. C. Poutsma, and R. N. Zare, *J. Phys. Chem. A* **102**, 9593 (1998).
- <sup>4</sup>W. T. Huntress and D. D. Elleman, *J. Am. Chem. Soc.* **92**, 3565 (1970).
- <sup>5</sup>W. T. Huntress, R. F. Pinizzotto, and J. B. Laudenslager, *J. Am. Chem. Soc.* **95**, 4107 (1973).
- <sup>6</sup>W. E. Conaway, T. Ebata, and R. N. Zare, *J. Chem. Phys.* **87**, 3447 (1987).
- <sup>7</sup>*NIST Chemistry WebBook*, edited by W. Mallard (NIST, <http://webbook.nist.gov/chemistry>, 1998), Vol. 69.
- <sup>8</sup>R. D. Guettler, G. C. Jones, L. A. Posey, N. J. Kirchner, B. A. Keller, and R. N. Zare, *J. Chem. Phys.* **101**, 3763 (1994).
- <sup>9</sup>L. A. Posey, R. D. Guettler, N. J. Kirchner, and R. N. Zare, *J. Chem. Phys.* **101**, 3772 (1994).
- <sup>10</sup>P. J. Miller, S. D. Colson, and W. A. Chupka, *Chem. Phys. Lett.* **145**, 183 (1988).
- <sup>11</sup>W. E. Conaway, R. J. S. Morrison, and R. N. Zare, *Chem. Phys. Lett.* **113**, 429 (1985).
- <sup>12</sup>D. Gerlich, *Adv. Chem. Phys.* **82**, 1 (1992).
- <sup>13</sup>J. C. Poutsma, M. A. Everest, J. E. Flad, G. C. Jones, and R. N. Zare, *Chem. Phys. Lett.* **305**, 343 (1999).
- <sup>14</sup>H. Fu, J. Qian, R. J. Green, and S. L. Anderson, *J. Chem. Phys.* **108**, 2395 (1998).